Available online at www.sciencedirect.com
SCIENCE DIRECT
ELSEVIER
International Journal of Multiphase Flow 32 (2006) 838–849
International Journal of Multiphase Flow
www.elsevier.com/locate/ijmulflow

Time scales for predicting dispersion of arbitrary-density particles in isotropic turbulence

Benoit Oesterlé [a,*], Leonid I. Zaichik [b]

[a] Lab. d'Energetique et de Mecanique Theorique et Appliquee (LEMTA), UMR 7563 CNRS, ESSTIN, Henri Poincaré University, 2 Rue Jean Lamour, 54500 Vandoeuvre-lés-Nancy, France
[b] Institute for High Temperatures of the Russian Academy of Sciences, Krasnokazarmennaya 17a, 111116 Moscow, Russia

Received 21 September 2005; received in revised form 16 February 2006

Abstract

The effects of particle inertia and particle-to-fluid density on the time scales that measure the dispersion of particles by isotropic turbulence are investigated. Numerical calculations are performed by means of a kinematic simulation method coupled with Lagrangian tracking of discrete particles. Moreover, a simple semi-empirical model for predicting the time scales of the fluid velocity seen by a particle as well as of the fluid–particle velocity covariance and the particle velocity variance is proposed. Comparisons between simulations and model predictions are presented.

Keywords: Particle dispersion; Time scales; Turbulence; Particle-to-fluid density ratio; Kinematic simulation

1. Introduction

The Lagrangian time scale of the fluid velocity seen by a particle (the so-called eddy–particle interaction time), T_{Lp}, is one of the most important parameters determining the dispersion of particles in a turbulent flow field. Therefore, a variety of works have been performed to investigate the effects of inertia and velocity drift of heavy particles on the eddy–particle interaction time scale. Hereafter the particles are considered as heavy if their material density is much higher than that of the fluid. It is well known that T_{Lp} coincides with the Lagrangian time scale of the turbulent fluid, T_{L}, only in the limit of zero-inertia particles. For inertial heavy particles, T_{Lp} may considerably differ from T_{L}, and, depending on inertia and drift parameters, $T_{\mathrm{Lp}}/T_{\mathrm{L}}$ can be greater or less than unity. In the absence of mean velocity drift between a particle and the fluid, T_{Lp} gradually increases from the Lagrangian to the Eulerian turbulence time scale, T_{E}, as the particle inertia increases (Reeks, 1977; Wang and Stock, 1993). In contrast, the mean velocity drift causes T_{Lp} to diminish (Yudine, 1959; Csanady, 1963). This phenomenon is spoken of in the literature as the ''crossing-trajectories effect''.

* Corresponding author. Tel.: +33 383 685 080; fax: +33 383 685 085.
E-mail address: benoit.oesterle@esstin.uhp-nancy.fr (B. Oesterlé).

0301-9322/$ - see front matter
doi:10.1016/j.ijmultiphaseflow.2006.02.011

In the present paper we investigate the effects of the particle inertia and the particle-to-fluid density ratio on the eddy–particle interaction time scale as well as on the integral time scales of fluid–particle velocity covariance and particle velocity variance. Numerical modeling is performed using the method of kinematic simulation of isotropic turbulence coupled with Lagrangian tracking of discrete particles. Additionally, a simple semi-empirical model is presented. This model is based on familiar Corrsin's hypothesis and valid for arbitrary-density inertial particles. Both simulations and predictions deal mainly with the large-scale velocity fluctuations and do not address the dynamics of small-scale turbulent eddies. The performance of the proposed simulations and analytical predictions is examined in the whole range of particle-to-fluid density ratio (from the case of heavy particles suspended in a gas to the situation of bubbles immersed in a liquid).

2. Kinematic simulation technique

Initiated by Kraichnan (1970), the kinematic simulation (KS) methods lie on the superposition of a large number of random Fourier modes in order to reproduce a homogeneous, isotropic, Gaussian turbulence. Such approaches are useful to examine some aspects connected with the behaviour of particles in a turbulent field at rather low cost, and with the advantage that velocity interpolation is not necessary in the process of particle tracking.

A divergence free velocity field is built according to the following truncated Fourier series for the local instantaneous velocity:

$$\mathbf{u}(\mathbf{x},t)=\sum_{n=1}^{N}[(\mathbf{a}_n\times\hat{\boldsymbol{\kappa}}_n)\cos(\boldsymbol{\kappa}_n\cdot\mathbf{x}+\omega_n t)+(\mathbf{b}_n\times\hat{\boldsymbol{\kappa}}_n)\sin(\boldsymbol{\kappa}_n\cdot\mathbf{x}+\omega_n t)], \tag{1}$$

where $\boldsymbol{\kappa}_n$ denotes the wavenumber vectors (with corresponding unit vectors $\hat{\boldsymbol{\kappa}}_n$), and ω_n is the frequency of the temporal mode associated to each spatial mode. The simplest way to define the parameters of the Fourier series is to randomly select the frequency ω_n and the components of the vectors $\mathbf{a}_n$, $\mathbf{b}_n$ and $\boldsymbol{\kappa}_n$ from zero mean Gaussian distributions with appropriate standard deviations to obtain the desired velocity variance $\langle u_i^2\rangle = u'^2$ and longitudinal integral length scale L. This method leads to the so-called Kraichnan spectrum, whose normalized expression ($u'=1$, $L=1$) is $E(\kappa)=(4/\pi^3)\kappa^4\exp(-\kappa^2/\pi)$ and which does not include any inertial range, so that the turbulence Reynolds number $Re_\mathrm{L}=u'L/\nu$ cannot be modified (ν is the fluid viscosity). Nevertheless, this technique was used by Maxey (1987) who was able to predict the turbulence induced increase in gravitational settling velocity of heavy particles, as well as by Wang and Stock (1992) in order to investigate the time scale of the fluid seen by heavy particles suspended in a homogeneous isotropic turbulence.

More recent KS techniques make it possible to simulate the inertial range and to vary the turbulence Reynolds number. Such techniques were developed mainly by Fung and his co-workers (e.g. Fung et al., 1992; Sakai et al., 1992), who proposed the KS Inertial Model, where the vectors $\mathbf{a}_n$ and $\mathbf{b}_n$ are selected to get an inertial range spectrum $E(\kappa)=C_K\varepsilon^{2/3}\kappa^{-5/3}$ for $\kappa_1\leqslant\kappa\leqslant\kappa_N$ and $E(\kappa)=0$ for $\kappa<\kappa_1$ or $\kappa>\kappa_N$ (κ_1 is the lowest wave number in the simulation, and ε is the dissipation rate of turbulent kinetic energy). The same authors proposed also the KS Sweeping Model, where large-scale modes are simulated by Markov processes and where the advection of small scales by large scales can be taken into account. The standard deviations of the components of $\mathbf{a}_n$ and $\mathbf{b}_n$ are selected to obtain the Von Karman spectrum

$$E(\kappa)=\gamma g_2\frac{\kappa^4}{(g_1+\kappa^2)^{17/6}}\quad\text{for } 0\leqslant\kappa\leqslant\kappa_N\quad\text{and}\quad E(\kappa)=0\quad\text{for }\kappa>\kappa_N, \tag{2}$$

which is close to $E(\kappa)=\gamma g_2\kappa^{-5/3}$ for large wavenumbers. Here, we adopt the same spectrum, but we assume that only the mean flow advects the small-scale eddies, a method that is simpler and less time consuming than the sweeping model. The unit vectors $\hat{\boldsymbol{\kappa}}_n$ are randomly selected with isotropic distribution. In the large-scale range, the wave numbers $\kappa_n=|\boldsymbol{\kappa}_n|$ are uniformly distributed from 0 to κ_c, where κ_c is a fixed cut-off wave number, whereas the small-scale wave numbers obey a geometric distribution from κ_c to κ_N, as suggested by Fung et al. (1992). In their KS models, the small-scale frequency modes ($\kappa_n>\kappa_\mathrm{c}$) are prescribed according to inertial scaling, i.e. $\omega_n=\lambda\varepsilon^{1/3}\kappa^{2/3}$, with the assumption $\lambda\varepsilon^{1/3}\approx 1$. In contrast, here the angular frequencies ω_n are randomly selected from a zero mean Gaussian distribution with given standard deviation σ_ω, a method that can

be shown to yield a semi-Gaussian Eulerian time correlation in a reference frame moving with the mean velocity, with integral time scale $T_E = \sigma_\omega^{-1}\sqrt{\pi/2}$. Therefore σ_ω determines the moving Eulerian time scale of the flow.

The spectrum $E(\kappa)$ and wave numbers are normalized in such a manner that $u' = 1$ and $L = 1$, or, equivalently,

$$\int_0^\infty E(\kappa)\mathrm{d}\kappa = \frac{3}{2} \quad \text{and} \quad \frac{3\pi}{4}\int_0^\infty \kappa^{-1}E(\kappa)\mathrm{d}\kappa = \frac{3}{2} \tag{3}$$

leading to $g_1 = 0.558$ and $g_2 = 1.196$ for $\gamma = 1$ in Eq. (2). Actually, due to the upper limitation in the wave number range, a slight correction has to be brought to the coefficient γ depending on the chosen value of κ_N, in order that $\int_0^{\kappa_N} E(\kappa)\mathrm{d}\kappa = \frac{3}{2}$. As a consequence, the integral length-scale L slightly differs from 1, but it can still be calculated exactly by $L = \frac{\pi}{2}\int_0^{\kappa_N} \kappa^{-1}E(\kappa)\mathrm{d}\kappa$.

In our computations, we fixed the normalized cut-off wave number at $\kappa_c = 5$, with six modes in the large-scale range, and we set $\sigma_\omega = 0.9$. The parameters of the simulated turbulence, which depend mainly on the maximum wave number κ_N, are then determined as follows:

- the dissipation rate of turbulent kinetic energy is given formally by $\varepsilon = 2\nu\int_0^\infty \kappa^2 E(\kappa)\mathrm{d}\kappa$. Here, the dissipative spectrum $2\nu\kappa^2E(\kappa)$ can only be integrated over the simulated wave number range, i.e. from 0 to κ_N. Therefore we can write $2\nu\int_0^{\kappa_N}\kappa E(\kappa)\mathrm{d}\kappa = \theta\varepsilon$, where $\theta < 1$ is a correction factor, and the Kolmogorov time scale of the simulated turbulence obeys

$$\tau_K = \left(\frac{\nu}{\varepsilon}\right)^{1/2} = \left(2\int_0^\infty \kappa^2 E(\kappa)\mathrm{d}\kappa\right)^{-1/2} = \left(\frac{2}{\theta}\int_0^{\kappa_N}\kappa^2E(\kappa)\mathrm{d}\kappa\right)^{-1/2}, \tag{4}$$

- the dissipation rate is estimated by equating the energy in the small-scale modes to the energy obtained by assuming that the spectrum in this range is nearly $C_K\varepsilon^{2/3}\kappa^{-5/3}$, with $C_K = 1.5$ (Fung et al., 1992):

$$C_K\varepsilon^{2/3}\int_{\kappa_c}^{\kappa_N}\kappa^{-5/3}\,\mathrm{d}\kappa \approx \int_{\kappa_c}^{\kappa_N} E(\kappa)\mathrm{d}\kappa, \tag{5}$$

- from Eqs. (4) and (5), the kinematic viscosity ν and the Kolmogorov length scale η can be expressed by

$$\nu = \varepsilon\tau_K^2 = \theta\varepsilon\left(2\int_0^{\kappa_N}\kappa^2E(\kappa)\mathrm{d}\kappa\right)^{-1}, \quad \eta = (\nu^3/\varepsilon)^{1/4}, \tag{6}$$

- the Taylor microscale λ_g is obtained from $\varepsilon = 15\nu u'2/\lambda_g^2$, which yields $\lambda_g = \sqrt{15}\tau_K u'$;
- finally, the Reynolds numbers Re_L and $Re_\lambda = u'\lambda_g/\nu$ of the simulated turbulence can be expressed in terms of the correction factor θ. The Reynolds number values given in the following are rough estimates obtained in assuming $\theta \cong 0.6$, keeping in mind that Re_L is inversely proportional to θ, and Re_λ is inversely proportional to $\sqrt{\theta}$.

In this paper, results are presented for two values of the estimated turbulence Reynolds number, namely $Re_L \cong 180$ ($Re_\lambda \cong 49$) and $Re_L \cong 1160$ ($Re_\lambda \cong 145$). The corresponding maximum wave numbers of the kinematic simulation are $\kappa_N = 16$ (with $N = 60$) and $\kappa_N = 65$ (with $N = 130$), respectively, leading to the values of the turbulence parameters shown in Table 1. In this table, the values of η/L can be verified to be very close to $Re_L^{-3/4}$, as it should be. The Lagrangian correlation functions and the corresponding Lagrangian time scale T_L have been computed from the statistics obtained by tracking 5×10^4 fluid particles, each in a different flow field

Table 1
Estimated parameters of the simulated turbulence

Re_L	Re_λ	$\varepsilon L/u'^3$	τ_K/T_L	η/L	λ_g/L	T_L/T_E
180	49	1.126	0.129	0.020	0.272	0.424
1160	145	0.832	0.059	0.0052	0.125	0.386

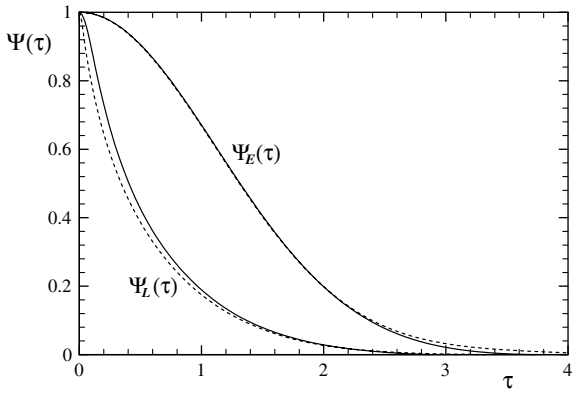

Fig. 1. The Lagrangian and Eulerian time correlation functions obtained by kinematic simulation: solid lines—$Re_\lambda \cong 49$; dashed lines—$Re_\lambda \cong 145$.

realization. Fig. 1 displays the Eulerian and Lagrangian autocorrelation functions resulting from the computed statistics.

3. Lagrangian tracking of particles

The motion of a single arbitrary-density particle at low Reynolds number (based on relative velocity and particle diameter) in a liquid (or gas) medium is governed by the equation

$$\frac{\mathrm{d}\mathbf{v}_\mathrm{p}}{\mathrm{d}t} = \frac{18\rho_\mathrm{f}\nu}{\rho_\mathrm{p} d^2}(\mathbf{u}-\mathbf{v}_\mathrm{p}) + \mathbf{g} + \frac{\rho_\mathrm{f}}{\rho_\mathrm{p}}\left(\frac{\mathrm{D}\mathbf{u}}{\mathrm{D}t} - \mathbf{g}\right) + C_\mathrm{A}\frac{\rho_\mathrm{f}}{\rho_\mathrm{p}}\left(\frac{\mathrm{D}\mathbf{u}}{\mathrm{D}t} - \frac{\mathrm{d}\mathbf{v}_\mathrm{p}}{\mathrm{d}t}\right), \tag{7}$$

where t is time, $\mathbf{v}_\mathrm{p}$ is the particle velocity, $\mathbf{u}$ is the carrier-flow velocity, ρ_f and ρ_p are the fluid and particle densities, d is the particle diameter, and $\mathbf{g}$ is the gravity acceleration. The terms on the right-hand side of (7) quantify, respectively, the viscous drag, the gravity force, the Archimedes displaced mass force, and the added mass force. The quasi-stationary drag force obeys the Stokes law, even for bubbles which can be considered as rigid particles in non-purified liquid, owing to interface contamination. Here, the Basset history force is neglected, although we are aware that it may play a significant role in case of particles which are not much denser than the fluid. Nevertheless, it is generally accepted that the effect of history force may also be neglected for very light particles like bubbles. The material derivative of the fluid velocity, $\mathrm{D}\mathbf{u}/\mathrm{D}t$, is evaluated along the trajectory of the surrounding fluid particle. Thus, the added mass force is written in the form proved by Auton et al. (1988) and Magnaudet et al. (1995) in contrast to Maxey and Riley (1983) who took the fluid velocity derivative in the added mass term along the trajectory of the inertial particle. For spherical particles the added mass factor, C_A, is equal to 0.5.

For the sake of convenience, Eq. (7) is rewritten as

$$\begin{aligned} &\frac{\mathrm{d}\mathbf{v}_\mathrm{p}}{\mathrm{d}t} = \frac{\mathbf{u}-\mathbf{v}_\mathrm{p}}{\tau_\mathrm{p}} + \alpha\mathbf{g} + \beta\frac{\mathrm{D}\mathbf{u}}{\mathrm{D}t}, \\ &\tau_\mathrm{p} = \left(\frac{\rho_\mathrm{p}}{\rho_\mathrm{f}} + \frac{1}{2}\right)\frac{d^2}{18\nu}, \quad \alpha = \frac{2(\rho_\mathrm{p}-\rho_\mathrm{f})}{\rho_\mathrm{f}+2\rho_\mathrm{p}}, \quad \beta = \frac{3\rho_\mathrm{f}}{\rho_\mathrm{f}+2\rho_\mathrm{p}}, \end{aligned} \tag{8}$$

where τ_p is the effective particle response time that allows for the added mass effect, α is the buoyancy parameter, and β is the particle-to-fluid density parameter. Finally, the following useful form of the equation of motion is obtained by introducing the unknown vector $\mathbf{v} = \mathbf{v}_\mathrm{p} - \beta\mathbf{u}$:

$$\frac{\mathrm{d}\mathbf{v}}{\mathrm{d}t} = -\mathbf{A}(\mathbf{v} - (1-\beta)\mathbf{u}) + \alpha\mathbf{g}, \tag{9}$$

where the components of the matrix $\mathbf{A}$ are $A_{ij} = \delta_{ij}/\tau_\mathrm{p} + \beta\partial u_i/\partial x_j$.

In this paper, numerical simulations of particle tracking are performed without gravity in order to focus in a first stage on the comparison with the analytical model predictions in the case of zero mean drift. The trajectories of many independent particles are computed without considering any effect of particle–particle interactions or of the dispersed phase upon the turbulence, by numerically integrating Eq. (9) together with the equation for the instantaneous particle location $\mathbf{R}_p$,

$$\frac{d\mathbf{R}_p}{dt} = \mathbf{v}_p = \mathbf{v} + \beta\mathbf{u} \tag{10}$$

by means of a third-order Runge–Kutta scheme. At each time step and particle location, the values of the fluid velocity components and their gradients (which are involved in the expression of the matrix $\mathbf{A}$) are deduced from the analytical expression (1). It should be noticed that Eq. (9) is not applicable for fluid particles ($\tau_p = 0$). In this case, i.e. in order to compute T_L, we used the following third-order Runge–Kutta scheme based on the equation $d\mathbf{x}/dt = \mathbf{u}(\mathbf{x}, t)$:

$$\mathbf{u}^n = \mathbf{u}(\mathbf{x}^n, t), \quad \tilde{\mathbf{u}}^{n+1/2} = \mathbf{u}\left(\mathbf{x}^n + \frac{1}{2}\mathbf{u}^n\Delta t, t + \frac{1}{2}\Delta t\right), \quad \tilde{\mathbf{u}}^{n+1} = \mathbf{u}(\mathbf{x}^n + (2\tilde{\mathbf{u}}^{n+1/2} - \mathbf{u}^n)\Delta t, t + \Delta t),$$

$$\mathbf{x}^{n+1} = \mathbf{x}^n + \frac{1}{6}(\mathbf{u}^n + 4\tilde{\mathbf{u}}^{n+1/2} + \tilde{\mathbf{u}}^{n+1})\Delta t,$$

where $\mathbf{x}$ denotes the fluid particle location, n is the initial time level and $n + 1$ is the final time level.

For each particle, a new turbulent field is generated and the initial location is randomly selected. The time step is chosen according to $\Delta t = \min(\tau_p/5,\ \tau_K/5)$, and the duration of each particle tracking is $t_{max} = \max(4T_L, 10\tau_p)$. The velocity correlations and corresponding time scales are computed from time $t = 5\tau_p$ to $t = t_{max}$, using at least 5×10^4 particles in as many different turbulent fields.

4. A model for predicting the time scales

4.1. The eddy–particle interaction time

In this section we present a simple semi-empirical model that incorporates the so-called inertia, crossing-trajectories, and continuity effects on the eddy–particle interaction time scale for arbitrary-density particles, that is, this model is valid in the whole range of the particle-to-fluid density parameter, β. To evaluate the Lagrangian time scale of the fluid velocity seen by a particle we invoke the familiar Corrsin hypothesis (Corrsin, 1959). This hypothesis enables the Lagrangian velocity correlation to be expressed through the Eulerian space–time correlations.

In homogeneous isotropic turbulence, the Lagrangian velocity correlation of a fluid element moving along a particle trajectory may be written as (Reeks, 1977)

$$\begin{aligned} B_{Lpij}(\tau) &= u'^2\Psi_{Lpij}(\tau) = \langle u_i'(\mathbf{x}, t)u_j'(\mathbf{R}_p(t-\tau), t-\tau)\rangle \\ &= \int \langle u_i'(\mathbf{x}, t)u_j'(\mathbf{x}-\mathbf{r}, t-\tau)\delta(\mathbf{r}-\mathbf{s}(\tau))\rangle d\mathbf{r}, \\ \mathbf{s} &= \mathbf{S} + \mathbf{s}', \quad \mathbf{S} = \mathbf{W}\tau, \quad \mathbf{s}' = \int_0^\tau \mathbf{v}_p'(\mathbf{R}_p(\tau_1))d\tau_1. \end{aligned} \tag{11}$$

Here $\Psi_{Lpij}(\tau)$ is the Lagrangian autocorrelation function of the fluid velocity seen by a particle, $\mathbf{R}_p$ is the particle position along its trajectory, $\mathbf{v}_p'$ is the particle fluctuating velocity, and u'^2 is the intensity of the fluid fluctuating velocity. In (11), the particle displacement relative to the moving fluid, $\mathbf{s}$, is presented as a sum of two independent processes, the first of them is a mean motion with the drift velocity $\mathbf{W} = \alpha\tau_p\mathbf{g}$ and the second is a fluctuating motion due to the particle response to velocity fluctuations of the turbulent fluid.

To determine (11) we use the Corrsin hypothesis that presumes independent averaging of the Eulerian random velocity field and the particle displacement. By this means (11) can be represented in the form

$$\begin{aligned} &\langle u_i'(\mathbf{x}, t)u_j'(\mathbf{x}-\mathbf{r}, t-\tau)\delta(\mathbf{r}-\mathbf{s}(\tau))\rangle = B_{Eij}(\mathbf{r}, \tau)\phi(\mathbf{r}, \tau), \\ &B_{Eij}(\mathbf{r}, \tau) = \langle u_i'(\mathbf{x}, t)u_i'(\mathbf{x}-\mathbf{r}, t-\tau)\rangle, \quad \phi(\mathbf{r}, \tau) = \langle\delta(\mathbf{r}-\mathbf{s}(\tau))\rangle, \end{aligned} \tag{12}$$

where $B_{\mathrm{E}ij}(\mathbf{r},\tau)$ is the second-order Eulerian space–time correlation of fluid velocities, and $\phi(\mathbf{r},\tau)$ denotes the probability of particle displacement over a distance $\mathbf{r}$ during time τ.

The displacement probability, $\phi(\mathbf{r},\tau)$, is usually approximated by a Gaussian distribution with a dispersion that is expressed through the Lagrangian autocorrelation function. In this case, (12) turns into an implicit nonlinear equation because $\Psi_{\mathrm{L}pij}(\tau)$ appears in both left and right parts. Therefore, the relevant equation may be solved only numerically or using iteration procedure. With a view to derive an explicit simple expression for $\Psi_{\mathrm{L}pij}(\tau)$, which may be easily used in the subsequent calculation, we approximate the displacement probability by the δ-function

$$\phi(\mathbf{r},\tau) = \delta(\mathbf{r} - \mathbf{s}(\tau)). \tag{13}$$

As is customary, the Eulerian spatial–temporal correlation moment is given by the product of the spatial and temporal correlations

$$\begin{aligned} &B_{\mathrm{E}ij}(\mathbf{r},\tau) = B_{ij}(\mathbf{r})\Psi_{\mathrm{E}}(\tau), \\ &B_{ij}(\mathbf{r}) = \langle u_i'(\mathbf{x},t)u_j'(\mathbf{x}-\mathbf{r},t)\rangle, \quad B_{ij}(0) = u'^2\delta_{ij}, \end{aligned} \tag{14}$$

where $B_{ij}(\mathbf{r})$ is the Eulerian spatial velocity correlation, and $\Psi_{\mathrm{E}}(\tau)$ is the Eulerian time autocorrelation function.

In homogeneous isotropic turbulence, the tensor $B_{ij}(\mathbf{r})$ can be written as

$$B_{ij}(\mathbf{r}) = u'^2\left\{G(r)\delta_{ij} + [F(r) - G(r)]\frac{r_i r_j}{r^2}\right\}, \quad G(r) = F(r) + \frac{r}{2}\frac{\mathrm{d}F(r)}{\mathrm{d}r}, \tag{15}$$

where $F(r)$ and $G(r)$ are the longitudinal and transverse components depending on the separation distance $r \equiv |\mathbf{r}|$. In (15), the latter relation stems from the continuity equation for isotropic turbulence.

Substituting (12)–(15) into (11) yields the following expression for the Lagrangian velocity autocorrelation function seen by a particle:

$$\begin{aligned} &\Psi_{\mathrm{L}pij}(\tau) = \left[G(S)\delta_{ij} + [F(S) - G(S)]\frac{\langle s_i s_j\rangle}{s^2}\right]\Psi_{\mathrm{E}}(\tau), \\ &\langle s_i s_j\rangle = W_i W_j\tau^2 + \langle s_i' s_j'\rangle, \quad s = \langle s_k s_k\rangle^{1/2}. \end{aligned} \tag{16}$$

The fluctuating component of particle displacement is evaluated from an approximate solution of the equation of motion (8), in which the derivative of the fluid velocity along the trajectory of the fluid particle is replaced by that along the trajectory of the inertial particle,

$$\frac{\mathrm{d}\mathbf{v}_{\mathrm{p}}'}{\mathrm{d}t} = \frac{\mathbf{u}'(\mathbf{R}_{\mathrm{p}},t) - \mathbf{v}_{\mathrm{p}}'}{\tau_{\mathrm{p}}} + \beta\frac{\mathrm{d}\mathbf{u}'}{\mathrm{d}t}. \tag{17}$$

From (17) it follows

$$\begin{aligned} \mathbf{s}' &= \int_0^{\tau}\left[\frac{1-\beta}{\tau_{\mathrm{p}}}\int_0^{\tau_1}\mathbf{u}'(\mathbf{R}_{\mathrm{p}}(\tau_2))\exp\left(-\frac{\tau_1-\tau_2}{\tau_{\mathrm{p}}}\right)\mathrm{d}\tau_2 + \beta\mathbf{u}'(\mathbf{R}_{\mathrm{p}}(\tau_1))\right]\mathrm{d}\tau_1 \\ &\approx \mathbf{u}_0'\left\{\tau + (1-\beta)\tau_{\mathrm{p}}\left[\exp\left(-\frac{\tau}{\tau_{\mathrm{p}}}\right) - 1\right]\right\}. \end{aligned} \tag{18}$$

The root mean square velocity, u', is taken as a characteristic fluctuating velocity of the fluid

$$|\mathbf{u}_0'| = u'. \tag{19}$$

According to (18) and (19) we obtain

$$\langle s_i' s_j'\rangle = \frac{u'^2\psi^2(\tau)}{3}\delta_{ij}, \quad \psi(\tau) = \tau + (1-\beta)\tau_{\mathrm{p}}\left[\exp\left(-\frac{\tau}{\tau_{\mathrm{p}}}\right) - 1\right]. \tag{20}$$

The quantity $u'\psi(\tau)$ is the effective free path of the particle in its fluctuating motion. As is clear, Eq. (16) along with (20) takes into account the "crossing-trajectories effect" induced by the drift velocity $\mathbf{W}$ as well as the

"inertia effect" that is qualified by both the particle response time τ_p and the particle-to-fluid density parameter β. It should be noted that approximation (16), which follows from (13), treats the particle displacement as a superposition of two processes: (i) the deterministic motion with the drift $\mathbf{W}$ and (ii) the random run with the dispersion specified by (20). Such an interpretation of the particle displacement in a turbulent flow is valid mainly at small time lag τ as compared to the integral time scale of turbulence when the velocity autocorrelation is close to unity. Errors introduced by these assumptions in predicting the time scales can be especially essential for large values of the structure parameter of the fluid turbulence $m \equiv T_E u'/L$, where T_E and L are the time and length macroscales. Therefore, the results obtained with the help of approximations (13), (16) and (20) should be thoroughly tested by comparison with numerical simulations.

In what follows, the Eulerian spatial and temporal correlations of the fluid turbulence are given by the exponential approximations

$$F(r) = \exp\left(-\frac{r}{L}\right), \quad \Psi_E(\tau) = \exp\left(-\frac{\tau}{T_E}\right). \tag{21}$$

Inserting (20) and (21) into (16) leads to the following expression for the Lagrangian velocity autocorrelation seen by a particle:

$$\Psi_{Lpij}(\tau) = \left\{\delta_{ij} + \frac{m[3\gamma^2\tau^2 e_i e_j - (3\gamma^2\tau^2 + 2\psi^2(\tau))\delta_{ij}]}{6(\gamma^2\tau^2 + \psi^2(\tau))^{1/2} T_E}\right\} \exp\left[-\frac{\tau + m(\gamma^2\tau^2 + \psi^2(\tau))^{1/2}}{T_E}\right]. \tag{22}$$

Here $\gamma \equiv W/u'$ is the drift parameter that measures the crossing-trajectories effect, $W \equiv |\mathbf{W}|$ is the drift magnitude, and $e_i \equiv W_i/W$ denotes the unit vector along the velocity drift.

When the mean drift is absent ($\gamma = 0$), the tensor $\Psi_{Lpij}(\tau)$ becomes isotropic

$$\Psi_{Lpij}(\tau) = \Psi_{Lp}(\tau)\delta_{ij},$$

where according to (22)

$$\Psi_{Lp}(\tau) = \left[1 - \frac{m\psi(\tau)}{3T_E}\right] \exp\left[-\frac{\tau + m\psi(\tau)}{T_E}\right]. \tag{23}$$

In the limit of zero-inertia particles ($\tau_p \to 0$), it follows from (23) and (20)

$$\Psi_L(\tau) = \left(1 - \frac{m\tau}{3T_E}\right) \exp\left[-\frac{(1+m)\tau}{T_E}\right]. \tag{24}$$

Eq. (24) determines the Lagrangian velocity autocorrelation function of the fluid turbulence. This produces the following simple relation between the Lagrangian and Eulerian integral time scales of the fluid turbulence:

$$\frac{T_L}{T_E} = \frac{3 + 2m}{3(1+m)^2}. \tag{25}$$

In the case of zero mean drift, the autocorrelation (23) yields the Lagrangian integral time scale of the fluid velocity seen by a particle in the form

$$T_{Lp} = \int_0^\infty \Psi_{Lp}(\tau)\mathrm{d}\tau = \int_0^\infty \left[1 - \frac{m\psi(\tau)}{3T_E}\right] \exp\left[-\frac{\tau + m\psi(\tau)}{T_E}\right]\mathrm{d}\tau. \tag{26}$$

It is clear that T_{Lp}/T_L is depending on three dimensionless parameters, namely, the Stokes number $St_E \equiv \tau_p/T_E$, the structure parameter m, and the particle-to-fluid density parameter β. In the limit of heavy particles ($\beta = 0$), T_{Lp} monotonically grows with increasing St_E from T_L at $St_E = 0$ up to T_E at $St_E = \infty$. When $\beta = 0$ and $m \leqslant 1$, the integral in Eq. (26) may be approximated by the relation

$$T_{Lp} = T_L + (T_E - T_L)\left[\frac{St_E}{1 + St_E} - \frac{0.9mSt_E^2}{(1+St_E)^2(2+St_E)}\right], \tag{27}$$

which asymptotically satisfies the limits for $St_E \to 0$, $St_E \to \infty$, and $m \to 0$.

In the case of low-inertia particles ($St_E \ll 1$), one can obtain

$$\frac{T_{Lp}}{T_L} = 1 + \left(\frac{T_E}{T_L} - 1\right)(\beta - 1)St_E + O(St_E^2).$$

In the opposite case of high-inertia particles ($St_E \to \infty$), (26) along with (20) leads to

$$\frac{T_{Lp}}{T_L} = \frac{(3 + 2m\beta)(1 + m)^2}{(3 + 2m)(1 + m\beta)^2}.$$

In accordance with (22), the Lagrangian integral time scales seen by a particle in the directions longitudinal and normal to the mean relative velocity, **W**, are given, respectively, as

$$T_{Lp}^{l} = \int_0^\infty \left[1 - \frac{m\psi^2(\tau)}{3(\gamma^2\tau^2 + 4\psi^2(\tau))^{1/2}T_E}\right] \exp\left[-\frac{\tau + m(\gamma^2\tau^2 + \psi^2(\tau))^{1/2}}{T_E}\right] d\tau, \tag{28}$$

$$T_{Lp}^{n} = \int_0^\infty \left[1 - \frac{m(3\gamma^2\tau^2 + 2\psi^2(\tau))}{6(\gamma^2\tau^2 + 4\psi^2(\tau))^{1/2}T_E}\right] \exp\left[-\frac{\tau + m(\gamma^2\tau^2 + \psi^2(\tau))^{1/2}}{T_E}\right] d\tau. \tag{29}$$

The distinction between T_{Lp}^{l} and T_{Lp}^{n} is the so-called continuity effect that stems from the continuity relation for the longitudinal and normal components of the velocity correlation in (15). When the crossing-trajectories effect is very strong ($\gamma \gg 1$), (28) and (29) yield, for any value of β, the well-known expressions of the time scales seen in the longitudinal and normal directions (Csanady, 1963)

$$T_{Lp}^{l} = \frac{L}{W}, \quad T_{Lp}^{n} = \frac{L}{2W}, \quad \frac{T_{Lp}^{l}}{T_{Lp}^{n}} = 2.$$

4.2. The time scale of fluid–particle velocity covariance

The Lagrangian fluid–particle velocity covariance moment is defined by

$$B_{fpij}(\tau) = < u_i'(\mathbf{x}, t)v_{pj}'(\mathbf{R}_p(t - \tau), t - \tau) >, \mathbf{R}_p(t) = \mathbf{x}. \tag{30}$$

The particle equation of motion (17) generates the following equation for the fluid–particle covariance (30):

$$\frac{dB_{fpij}}{d\tau} - \frac{B_{fpij}}{\tau_p} = -\frac{B_{Lpij}}{\tau_p} + \beta\frac{dB_{Lpij}}{d\tau}, \tag{31}$$

where $B_{Lpij}(\tau)$ is the Lagrangian fluid velocity correlation seen by a particle, see Eq. (11). By making use of matrix notation, the solution of (31) that satisfies $B_{fpij} \to 0$ for $\tau \to \infty$ may be written as

$$\begin{aligned}\mathbf{B}_{fp}(\tau) &= \frac{1 - \beta}{\tau_p}\int_\tau^\infty \mathbf{B}_{Lp}(\xi)\exp\left(\frac{\tau - \xi}{\tau_p}\mathbf{I}\right)d\xi + \beta\mathbf{B}_{Lp}(\tau) \\ &= u'^2\left[\frac{1 - \beta}{\tau_p}\int_\tau^\infty \mathbf{\Psi}_{Lp}(\xi)\exp\left(\frac{\tau - \xi}{\tau_p}\mathbf{I}\right)d\xi + \beta\mathbf{\Psi}_{Lp}(\tau)\right] = u'^2\mathbf{F}_{fp}(\tau),\end{aligned} \tag{32}$$

where **I** denotes the unit matrix.

The integral time scale of fluid–particle covariance is defined as

$$\mathbf{T}_{fp} = \mathbf{F}_{fp}^{-1}(0)\int_0^\infty \mathbf{F}_{fp}(\tau)d\tau = \mathbf{F}_{fp}^{-1}(0)(\mathbf{T}_{Lp} + \beta\tau_p\mathbf{I}) - \tau_p\mathbf{I}. \tag{33}$$

If the Lagrangian fluid velocity autocorrelation seen by a particle is taken in the form of the exponential approximation

$$\Psi_{Lp}(\tau) = \exp(-\tau\mathbf{T}_{Lp}^{-1}), \tag{34}$$

the fluid–particle covariance function (32) is represented as

$$\mathbf{F}_{\mathrm{fp}}(\tau) = (\mathbf{T}_{\mathrm{Lp}} + \tau_{\mathrm{p}}\mathbf{I})^{-1}(\mathbf{T}_{\mathrm{Lp}} + \beta\tau_{\mathrm{p}}\mathbf{I})\exp(-\tau\mathbf{T}_{\mathrm{Lp}}^{-1}). \tag{35}$$

Substitution of (35) into (33) gives that the integral time scale of fluid–particle covariance is equal to the eddy–particle interaction time scale

$$\mathbf{T}_{\mathrm{fp}} = \mathbf{T}_{\mathrm{Lp}}.$$

4.3. The time scale of particle velocity variance

The Lagrangian particle velocity variance moment is defined by

$$B_{\mathrm{p}ij}(\tau) = < v'_{\mathrm{p}i}(\mathbf{x},t)v'_{\mathrm{p}j}(\mathbf{R}_{\mathrm{p}}(t-\tau),t-\tau) >, \mathbf{R}_{\mathrm{p}}(t) = \mathbf{x}. \tag{36}$$

The particle equation of motion (17) produces the following equation for the particle variance moment (36):

$$\frac{\mathrm{d}^2 B_{\mathrm{p}ij}}{\mathrm{d}\tau^2} - \frac{B_{\mathrm{p}ij}}{\tau_{\mathrm{p}}^2} = -\frac{B_{\mathrm{Lp}ij}}{\tau_{\mathrm{p}}^2} + \beta^2\frac{\mathrm{d}^2 B_{\mathrm{Lp}ij}}{\mathrm{d}\tau^2}. \tag{37}$$

The solution of (37) that satisfies the boundary conditions

$$\frac{\mathrm{d}B_{\mathrm{p}ij}}{\mathrm{d}\tau} = 0 \quad \text{for } \tau = 0, \qquad B_{\mathrm{p}ij} \to 0 \quad \text{for } \tau \to \infty$$

is given by

$$\begin{aligned}\mathbf{B}_{\mathrm{p}}(\tau) &= u'^2\left\{\frac{1-\beta^2}{2\tau_{\mathrm{p}}}\int_0^\infty\left[\exp\left(-\frac{|\tau+\xi|}{\tau_{\mathrm{p}}}\mathbf{I}\right) + \exp\left(-\frac{|\tau-\xi|}{\tau_{\mathrm{p}}}\mathbf{I}\right)\right]\mathbf{\Psi}_{\mathrm{Lp}}(\xi)\mathrm{d}\xi + \beta^2\mathbf{\Psi}_{\mathrm{Lp}}(\tau)\right\} \\ &= u'^2\mathbf{F}_{\mathrm{p}}(\tau).\end{aligned} \tag{38}$$

The integral time scale of particle velocity is defined by

$$\mathbf{T}_{\mathrm{p}} = \mathbf{F}_{\mathrm{p}}^{-1}(0)\int_0^\infty \mathbf{F}_{\mathrm{p}}(\tau)\mathrm{d}\tau = \mathbf{F}_{\mathrm{p}}^{-1}(0)\mathbf{T}_{\mathrm{Lp}}. \tag{39}$$

If the Lagrangian fluid velocity autocorrelation seen by a particle obeys Eq. (34), then the particle velocity correlation function takes the form

$$\begin{aligned}\mathbf{F}_{\mathrm{p}}(\tau) = \frac{1-\beta^2}{2}\Bigg\{&(\mathbf{I}+\tau_{\mathrm{p}}\mathbf{T}_{\mathrm{Lp}}^{-1})^{-1}\left[\exp(-\tau\mathbf{T}_{\mathrm{Lp}}^{-1}) + \exp\left(-\frac{\tau}{\tau_{\mathrm{p}}}\mathbf{I}\right)\right] \\ &+(\mathbf{I}-\tau_{\mathrm{p}}\mathbf{T}_{\mathrm{Lp}}^{-1})^{-1}\left[\exp(-\tau\mathbf{T}_{\mathrm{Lp}}^{-1}) - \exp\left(-\frac{\tau}{\tau_{\mathrm{p}}}\mathbf{I}\right)\right]\Bigg\} + \beta^2\exp(-\tau\mathbf{T}_{\mathrm{Lp}}^{-1})\end{aligned}$$

and hence

$$\mathbf{F}_{\mathrm{p}}(0) = (\mathbf{I}+\tau_{\mathrm{p}}\mathbf{T}_{\mathrm{Lp}}^{-1})^{-1}(\mathbf{I}+\beta^2\tau_{\mathrm{p}}\mathbf{T}_{\mathrm{Lp}}^{-1}). \tag{40}$$

Substituting (40) into (39) yields the following formula for the particle time scale:

$$\mathbf{T}_{\mathrm{p}} = (\mathbf{I}+\tau_{\mathrm{p}}\mathbf{T}_{\mathrm{Lp}}^{-1})(\mathbf{I}+\beta^2\tau_{\mathrm{p}}\mathbf{T}_{\mathrm{Lp}}^{-1})^{-1}\mathbf{T}_{\mathrm{Lp}}. \tag{41}$$

With no mean drift ($\mathbf{W} = 0$), $\mathbf{T}_{\mathrm{Lp}} = T_{\mathrm{Lp}}\mathbf{I}$ and thus the particle time scale is a scalar rather than a tensor. In this case, Eq. (41) shows that the impact of particle inertia on T_{p} depends on the value of β. In perfect analogy to T_{Lp}, T_{p} increases or decreases with τ_{p} for $\beta < 1$ or $\beta > 1$.

5. Simulation and prediction results

Relation (25) predicts that in isotropic turbulence the Lagrangian-to-Eulerian time scale ratio is only a function of the turbulence structure parameter m. Fig. 2 illustrates this function. In Fig. 2, some theoretical

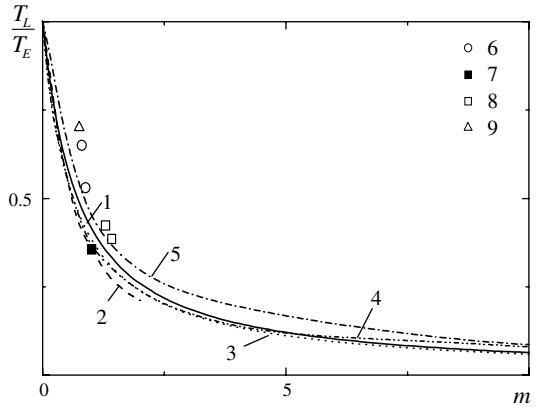

Fig. 2. The Lagrangian-to-Eulerian time scale ratio against the turbulence structure parameter: 1—Eq. (25), 2—Philip (1967), 3—Lee and Stone (1983), 4—Stepanov (1996), 5—Derevich (2001), 6—Fung et al. (1992), 7—Wang and Stock (1993), 8—present simulations, 9—Mazzitelli and Lohse (2004).

dependences and numerical data known from the literature are also shown. It is seen that Eq. (25) is in qualitative agreement with all the data presented.

Fig. 3 presents the eddy–particle interaction time for heavy particles ($\beta = 0$). Predictions are performed for $m = 1$, but the simulations relate to somewhat greater values of m. As is seen, the simulation data compare favourably with the known correlation proposed by Wang and Stock (1993)

$$T_{\mathrm{Lp}} = \left[1 - \frac{0.644}{(1 + St_{\mathrm{E}})^{0.4(1+0.01St_{\mathrm{E}})}}\right] T_{\mathrm{E}}, \quad \frac{T_{\mathrm{L}}}{T_{\mathrm{E}}} = 0.356. \tag{42}$$

It can be observed that Eqs. (26) and (27) are very close even for $m = 1$, however they do not match the numerical simulations as well as Eq. (42). The simulation results indicate that the influence of the Reynolds number on $T_{\mathrm{Lp}}/T_{\mathrm{L}}$ is quite weak.

Eq. (26) along with (20) predicts that, with increasing particle response time, T_{Lp} monotonically increases for particles which are heavier than the carrier fluid ($\beta < 1$) and decreases for particles which are lighter than the carrier fluid ($\beta > 1$). The decrease in the eddy–particle interaction time for lighter particles is due to the enhancement of their mobility with increasing Stokes number, as shown by Eq. (40). Owing to that, the fluid velocity correlation defined along a particle path diminishes and hence T_{Lp} decreases. When the density of

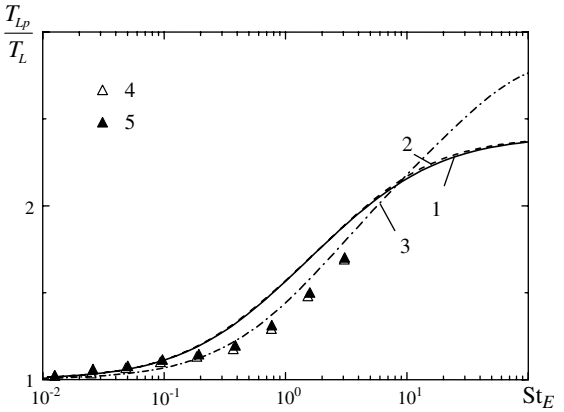

Fig. 3. Effect of the Stokes number on the eddy–particle interaction time for heavy particles: 1—Eq. (26); 2—Eq. (27); 3—Eq. (42); 4, 5—simulations; 4—$Re_\lambda \cong 49$ and $m = 1.14$; 5—$Re_\lambda \cong 145$ and $m = 1.29$.

both phases are equal ($\beta = 1$), $T_{\mathrm{Lp}} = T_{\mathrm{L}}$ for all values of St_{E}. Fig. 4 shows the effect of particle inertia on the eddy–particle interaction time scale seen by a particle for various particle-to-fluid densities. Here the particle

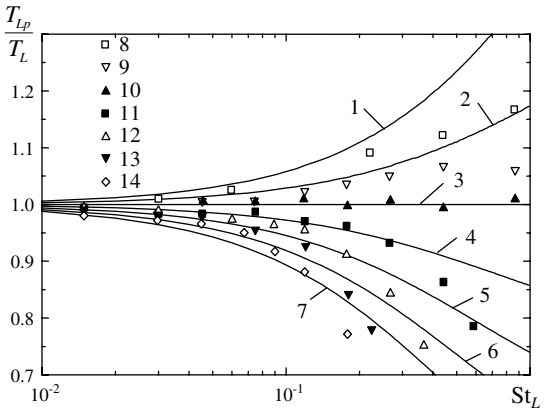

Fig. 4. The eddy–particle interaction time as a function of the Stokes number and the particle-to-fluid density parameter at $Re_\lambda \cong 49$: 1–7—model predictions; 8–14—numerical simulations; 1,8—$\beta = 0$; 2, 9—0.5; 3, 10—1.0; 4, 11—1.5; 5,12—2.0; 6,13—2.5; 7,14—3.0.

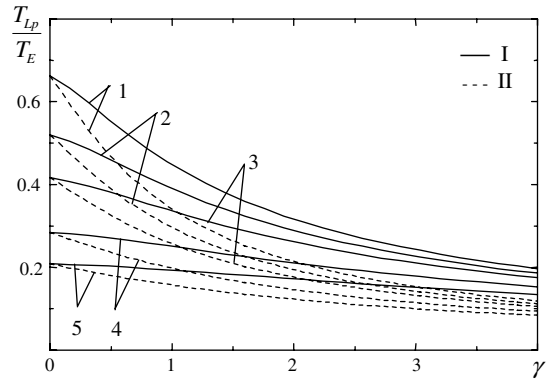

Fig. 5. Effect of the drift parameter on the eddy–particle interaction time in the directions longitudinal (I) and normal (II) to the mean relative velocity vector: I—Eq. (28), II—Eq. (29), 1–5—$\beta = 0$, 0.5, 1, 2, 3.

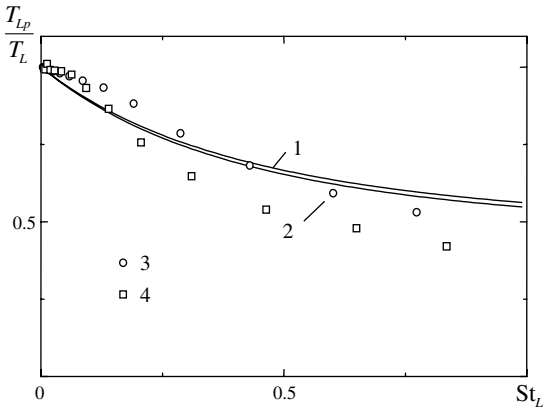

Fig. 6. Effect of the Stokes number on the eddy–bubble interaction time scale for $\beta = 3$: 1,2—model predictions; 3,4—numerical simulations; 1,3—$Re_\lambda \cong 49$; 2,4—$Re_\lambda \cong 145$.

inertia is quantified by the Stokes number $St_L \equiv \tau_p/T_L$ based on the Lagrangian time scale. As is clear from Fig. 4, the model predictions and the numerical simulations are in full qualitative agreement.

The influence of the crossing-trajectories effect on the eddy–particle interaction times is illustrated in Fig. 5. The predictions are appropriate to Eqs. (28) and (29) for $m = St_E = 1$. It is clear that, for all values of β, an increase in the drift results in a decrease in the eddy–particle interaction time. Thus, increasing the particle-to-fluid density parameter or the drift parameter results in a qualitatively similar effect on the eddy–particle interaction time scales.

Fig. 6 presents the influence of the Stokes number on the Lagrangian time scale of the fluid velocity seen by a bubble (the eddy–bubble interaction time scale) for $\beta = 3$. As is evident from comparison of Figs. 3 and 6, the effect of the Stokes number on T_{Lp} for heavy particles and light bubbles is directly opposite.

6. Summary

The effects of particle inertia and particle-to-fluid density ratio upon the time scales that quantify the particle dispersion in homogeneous isotropic turbulence have been investigated by means of kinematic simulation. Furthermore, a semi-empirical model, taking into account the inertia, crossing-trajectories and continuity effects for arbitrary-density particles, has been developed. The results of the numerical simulations and the model predictions are found to be in encouraging agreement.

The main finding drawn from the simulations and the analytical model is the directly opposite influence of particle inertia upon the eddy–particle interaction time scale for heavy and light particles. Rather than increasing as for heavy particles ($\beta < 1$), the eddy–particle interaction time decreases with increasing response time of light particles or bubbles ($\beta > 1$). The model predicts that the effect of crossing-trajectories for heavy and light particles is qualitatively similar and results in a monotonous decrease in the eddy–particle interaction time scales for all values of the particle-to-fluid density parameter.

As a next step in the investigation of times scales that measure the turbulent dispersion of arbitrary-density particles, we are going to simulate numerically the crossing-trajectories effect for light particles and bubbles to check the model predictions presented in Fig. 5.

References

Auton, T.R., Hunt, J.C.R., Prud'homme, M., 1988. The force exerted on a body in inviscid unsteady non-uniform rotational flow. J. Fluid Mech. 197, 241–257.

Corrsin, S., 1959. Progress report on some turbulent diffusion research. Adv. Geophys. 6, 161–184.

Csanady, G.T., 1963. Turbulent diffusion of heavy-particles in the atmosphere. J. Atmos. Sci. 20, 201–208.

Derevich, I.V., 2001. Influence of internal turbulent structure on intensity of velocity and temperature fluctuations of particles. Int. J. Heat Mass Transfer 44, 4505–4521.

Fung, J.C.H., Hunt, J.C.R., Malik, N.A., Perkins, R.J., 1992. Kinematic simulation of homogeneous turbulence by unsteady random Fourier modes. J. Fluid Mech. 236, 281–318.

Kraichnan, R.H., 1970. Diffusion by a random velocity field. Phys. Fluids 13, 22–31.

Lee, J.T., Stone, G.L., 1983. Eulerian–Lagrangian relationships in Monte Carlo simulations of turbulent diffusion. Atmos. Environ. 17, 2483–2487.

Magnaudet, J., Rivero, M., Fabre, J., 1995. Accelerated flows past a rigid sphere or a spherical bubble. Part 1. Steady straining flow. J. Fluid Mech. 284, 97–135.

Maxey, M.R., 1987. The gravitational settling of aerosol particles in homogeneous turbulence and random flow fields. J. Fluid Mech. 174, 441–465.

Maxey, M.R., Riley, J., 1983. Equation of motion for a small rigid sphere in a non uniform flow. Phys. Fluids 26, 883–889.

Mazzitelli, I.M., Lohse, D., 2004. Lagrangian statistics for fluid particles and bubbles in turbulence. New J. Phys. 6, 1–28.

Philip, J.R., 1967. Relations between Eulerian and Lagrangian statistics. Phys. Fluids. (Supplement) 10, S69–S71.

Reeks, M.W., 1977. On the dispersion of small particles suspended in an isotropic turbulent fluid. J. Fluid Mech. 83, 529–546.

Sakai, Y., Hunt, J.C.R., Fung, J.C.H., 1992. Diffusion of fluid particles by the combined model of random Fourier modes and random flight. JSME Int. J. II-35, 497–506.

Stepanov, A.S., 1996. On relation between Eulerian and Lagrangian turbulence correlations. Meteorol. Hydrol. 5, 50–59.

Wang, L.-P., Stock, D.E., 1992. Numerical simulation of heavy particle dispersion: time step and nonlinear drag considerations. J. Fluids Eng. 114, 100–106.

Wang, L.-P., Stock, D.E., 1993. Dispersion of heavy particles by turbulent motion. J. Atmos. Sci. 50, 1897–1913.

Yudine, M.I., 1959. Physical consideration on heavy-particle dispersion. Adv. Geophys. 6, 185–191.